Shear Testing of Al and Al-Al_4C_3 Materials at Elevated Temperatures

Vasilios Spitas [1], *Michal Besterci [2], Paul Michelis [3], Christos Spitas [4]

[1] *Technical University of Crete, Applied Mechanics Laboratory, Akrotiri Campus, 73100, Chania, Greece*

[2] *Institute of Materials Research, Slovak Academy of Sciences, Watsonova 47, Kosice 04353, Slovakia*

[3] *Institute of Mechanics of Materials and Geostructures, 22 Askiton Str., Penteli 15236, Greece*

[4] *National Technical University of Athens, Machine Elements Lab., 7 Iroon Polytechniou Str., Athens, Greece.*

(Received March 24, 2004; final form April 10, 2004)

ABSTRACT

The shear creep properties of the Al–Al_4C_3 composite material were investigated for the first time at different temperatures ranging from 523 K to 773 K and different shear stress levels ranging from 25 to 40 MPa in comparison to pure aluminum. The specimens were loaded in pure shear using a specially designed patented specimen geometry and a prototype shear-testing machine. The experimental results indicate that the Al_4C_3 composite aluminum exhibits shear creep resistance more than four orders of magnitude higher than that of the unalloyed aluminum and can be loaded at shear stress levels exceeding two times those of the pure aluminum material.

Keywords: Shear creep testing, Al, Al-Al_4C_3 composite, elevated temperature, F.E. analysis

1. INTRODUCTION

The dispersion strengthened alloys Al–Al_4C_3 manufactured by mechanical alloying using powder metallurgy technology are promising structural materials enabling significant reductions of weight for use first of all in the aircraft and automobile industry and also at elevated temperatures.

Although the properties of such alloys in simple tension have been thoroughly investigated at room and elevated temperatures /1-5/ where they have demonstrated their superior mechanical properties as compared with the pure aluminum, there has not been any work in shear and particularly shear–creep properties at elevated temperatures. The behaviour of this material in shear is of critical importance as most aluminum materials used in the aerospace and automotive industry (in the form of thin shells or bulk materials such as internal combustion machines pistons) is subjected to considerable shear either as torsion or mixed biaxial or triaxial loading. Shear creep of several composite materials was analyzed in /6-11/.

In the present work the alloy Al–Al_4C_3 is tested in shear at elevated temperatures ranging from 523 K to 773 K under creep conditions in comparison to standard pure aluminum specimens. All testing is conducted in a prototype shear testing machine, which uses patented specimen geometry /12/ based on the Iosipescu shear testing array /13,14/. The selected specimen geometry and testing machine is able to provide pure shear

* Corresponding Author, e-mail: besterci@imrnov.saske.sk

conditions (i.e. with zero normal stress) in the central region (gauge area) of the specimen.

The results indicate the supremacy of this alloy (some orders of magnitude in terms of creep resistance) compared to the standard unalloyed structural aluminum. Also higher stress levels (up to two times more) are attainable.

2. SHEAR TESTING AT ELEVATED TEMPERATURE

The shear specimen used for the shear tests in pure aluminum and Al–Al_4C_3 (Metal Matrix Composite) is illustrated in Fig. 1. The geometry of the specimen and particularly the central (gauge) area of the specimen are composed of a smooth U–groove in the shear plane and a ramp waste profile in the transverse (out of the shear plane) direction.

The analysis has illustrated that when the specimen is loaded with the pair of opposite forces on the outer pin-holes illustrated in Fig. 1, then these externally applied forces along with the pair of reactions developed on the inner stationary pins generate pure shear loading (i.e. with no tension or bending) along the gauge area of the specimen.

The testing machine used to generate the uniform shear field on the specimens is the shear machine illustrated in Fig. 2. This machine is a single axis servo-hydraulic one that is capable of applying shear forces up

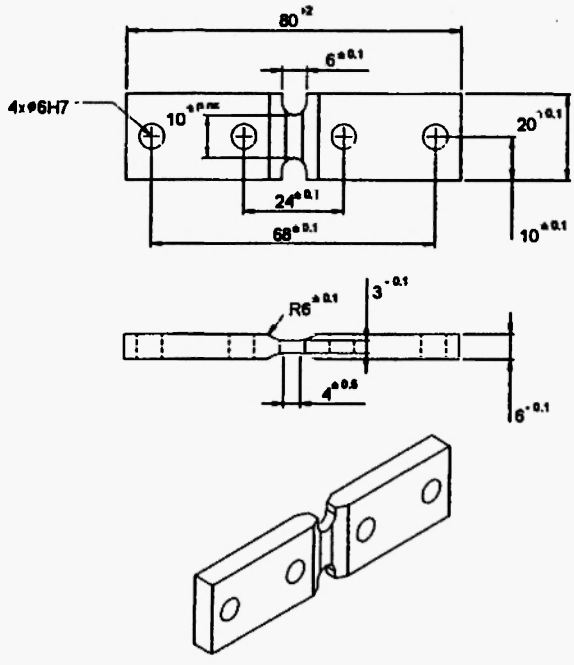

Fig. 1: The shear specimen

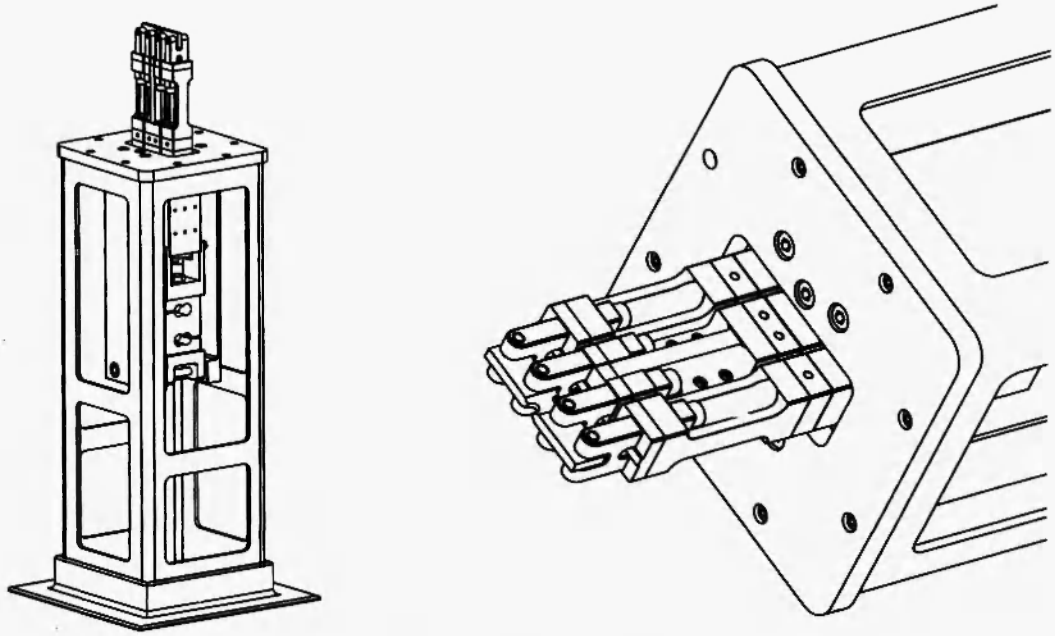

Fig. 2: Shear machine overview and gripping system detail

to 15 kN at the central region of the above – presented shear specimen. Only the central region of the specimen is loaded in shear and therefore all stress-strain measurements refer to this part of the sample.

The shear machine is composed of two stationary inner grips and two moving outer grips identical to the stationary ones for securely clamping the specimen with the help of four precise pins. The grips made of the heat resistant superalloy NIMONIC 115 are insulated by two plates of fused alumina and connected to the machine body and the moving arms respectively with eight identical hexagonal socket-type bolts. In order to prevent damage to the sensitive electronic and hydraulic parts of the machine, the heat flow at the lower end of the arms (both moving and stationary) is absorbed from three bronze water coolers. The two outer moving arms are connected with two special double-acting hydraulic pistons operating under 300 bar maximum hydraulic pressure. The forces developed by the two pistons on the specimen are measured using two shear web–type load cells and their direction is self-aligned to the perpendicular to the deformed central axis of the specimen by means of a free rotating pivot at the axis end.

The heating of the specimen up to 1273 K is realized using a furnace at the top of the shear machine. This oven includes the specimen and the grips and uses a KANTHAL superheating element able to reach temperatures up to 1873 K. The achieved temperature field of the specimen (crack zone) is almost uniform (difference in temperature over the central zone less than 1.5%). Since the heating elements heat the specimen from all sides, the furnace is large in comparison with the specimen and the loading train is thermally insulated by alumina thermal barriers. Also the temperature is kept constant (±277 K) over time using a control system with two thermocouples mounted on both sides of the specimen. The atmosphere of the furnace can be either oxidizing or vacuum. The observation of the specimen at high temperature is made possible by the use of a window on the oven covered with special temperature resistant sapphire glass.

3. FINITE ELEMENT ANALYSIS OF THE SHEAR SPECIMEN

In order to verify that a pure shear field is developed in the gauge area of the specimen, numerical analysis using FEM was carried out using tetrahedral isoparametric finite elements in the elastic domain. The loading of the shear specimen was modeled as a uniformly distributed load on the load bearing inner surface of the outer pinholes and the inner pins were modeled as supports allowing free rotation but no linear motion.

The specimen loading conditions are illustrated in Fig. 3. It is evident that under the externally applied pair of forces F_1 from the outer grips the pair of reactions F_2 are developed at the inner grips and the shear force at the center of the specimen is $F_2 - F_1$. Due to the specially designed U-grooves and the smooth recess at the central portion of the specimen the developed stress field there is uniform with negligible tensile or compressive stress component (pure shear).

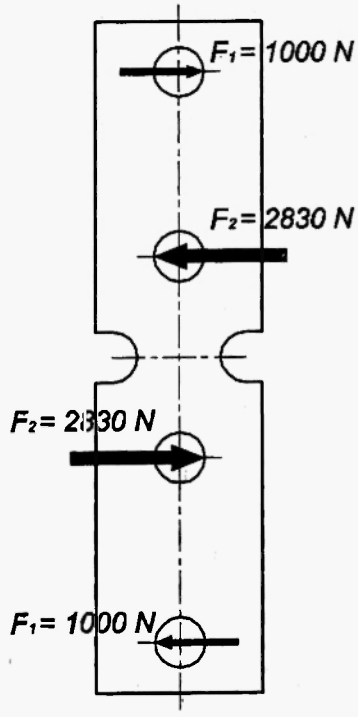

Fig. 3: Loading conditions of the shear specimen

The average (mean) shear stress τ_m developed at the gage area of the specimen is calculated from the following equation:

$$\tau_m = \frac{F_2 - F_1}{A} \quad (1)$$

where A is the cross section of the specimen gage area. For a shear specimen of standard geometry $A = 30mm^2$ and $F_2 = F_1 \times \frac{68}{24} = 2.83 \times F_1$.

The shear field is characterized by zero shear stress at the U groove boundaries and constant maximum shear stress at the central area of the specimen whereas the normal stresses are equal to zero at the center as illustrated in Figs. 4 and 5.

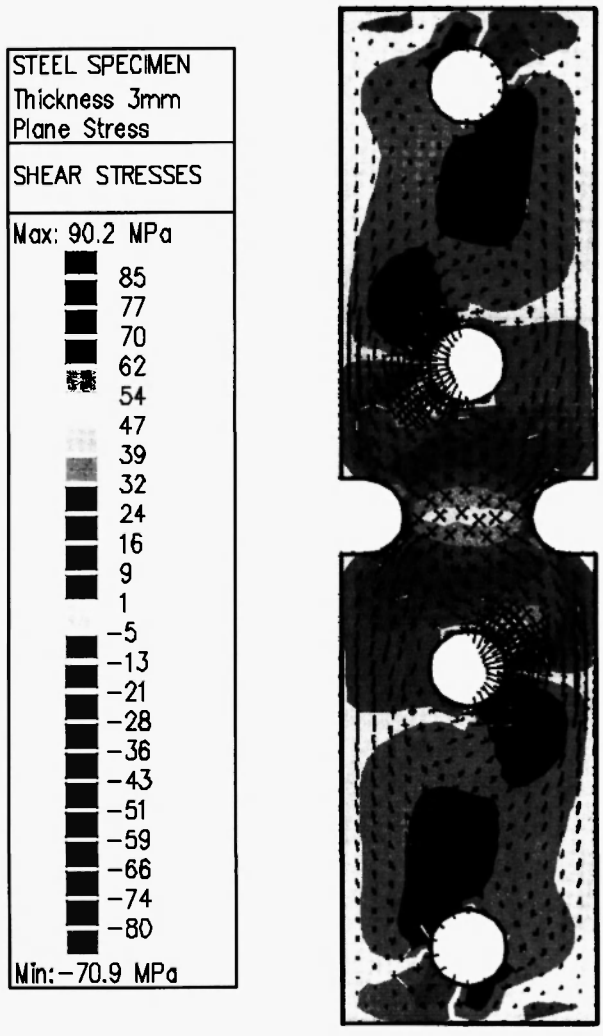

Fig. 4: Shear stress field superimposed on principal stress vector field

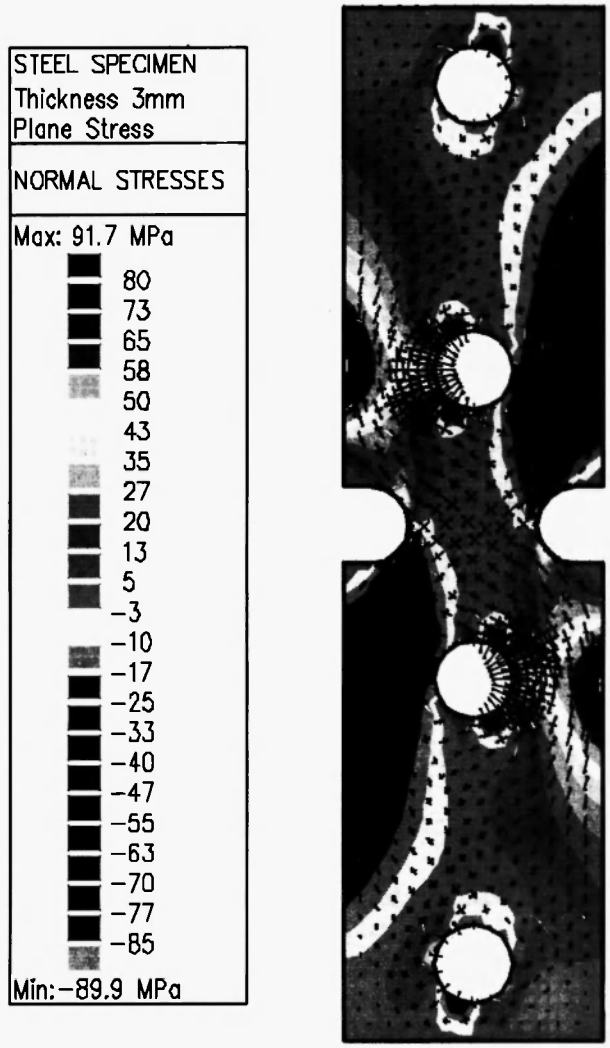

Fig. 5: Normal stress field superimposed on principal stress vector field

4. SHEAR DEFORMATION MEASURING TECHNIQUES AT HIGH TEMPERATURES

In order to facilitate image processing at high temperatures where the surface of the specimen is oxidized, distinctive marks on the gage area of the specimen must be created. These marks should not affect the mechanical properties of the material or induce stress concentrations and at the same time they must be clearly visible at high temperature (i.e. create high contrast with the base material) and be unaffected by the oxidizing environment. The blurring of the image due to convection was eliminated by taking the images

at reduced pressure (vacuum) in the order of a few millibars using two piston air pumps and a vacuum chamber.

The first technique employed on the aluminum based materials was to print a grid of squares or rectangles, using gold sputtering, directly onto the surface of the specimen. The specimen was masked with a grid of 50 μm x 50 μm squares with 10 μm spacing and the image acquired from the microscope was processed in false colour (Fig. 6) for measuring deformation.

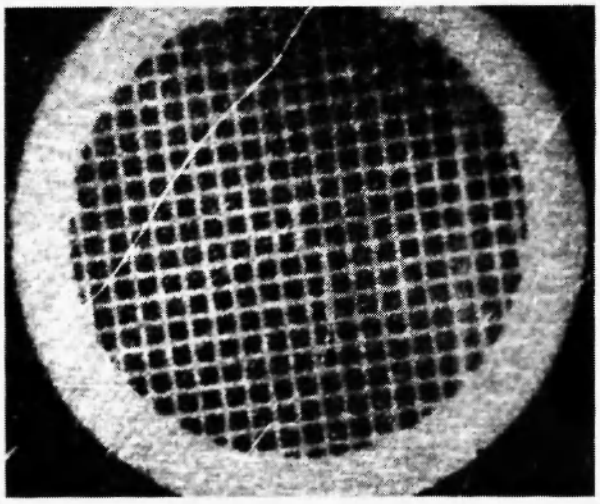

Fig 6: Gold sputtered grid for measuring deformation

Disadvantages of this method include the difficulty in obtaining sharp grid boundaries, due to the fact that the sputtering technique allows for atoms to penetrate the mask and make irregular deposits along the grid boundaries, therefore creating diffuse images and introducing considerable errors in the optical measurements. It should also be noticed that the large plastic deformations attributed to the superplastic behaviour of the examined materials at elevated temperatures led to heavily distorted images where no post processing could be made.

The second and so far more successful technique employed was to engrave a grid of conical holes about ∅50μm x 50 μm deep directly onto the specimen using a suitable carbide indentation tool. On the images acquired from the optical microscope at high temperature the hole boundaries are sharp and well defined and therefore the changes in their relative position can be monitored and the deformations either in shear or tension / compression can be measured hence the strain field is evaluated.

Figure 7 illustrates part of this grid engraved on aluminum at 773 K under some shear deformation. The image processing is carried out on the Autodesk MAP 2004 GIS image processing software platform. On each hole a polygon is drawn by the user along its boundaries and the centroid of this polygon is calculated automatically by the software. Distances between centroids and angles can be measured using this software with an accuracy of ~ 2 – 3 μm.

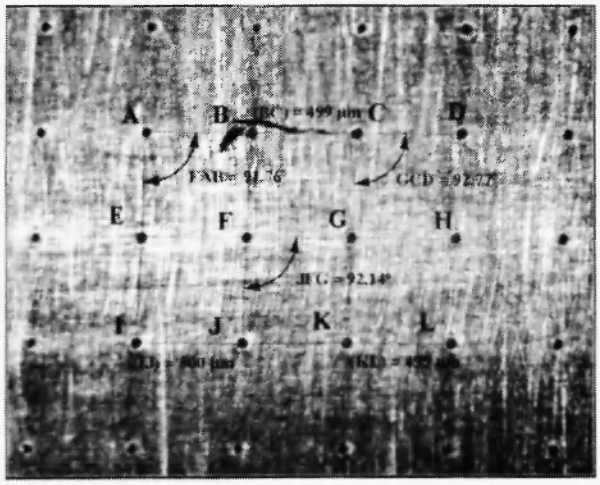

Fig. 7: Deformation measurement with engraved holes on the specimen

5. EXPERIMENTAL RESULTS AND DISCUSSION

Six specimens from pure aluminum and one specimen from aluminum matrix carbide alumina produced by mechanical alloying were tested in comparison under different shear loading and temperature. On all specimens the aforementioned grid of holes was engraved and the changes of the grid pattern were recorded at successive time intervals using an optical long distance observation microscope. From image analysis the strain maps were produced and the

creep rates were calculated.

The test matrix and the experimental shear creep conditions of the aluminum specimens are presented in the table below along with the time to fracture. All specimens from pure unalloyed aluminum exhibited the classical three–stage creep behaviour, i.e. a linear stage I where the creep was advancing rapidly, a stable stage II where the creep was advancing at constant rate and a rapidly increasing final stage which led them to failure. In the diagrams presented in Figs. 8–12 stages II and III and fitted linear regressions are presented for all pure Al specimens except for specimen No. 4 (see Table 1) which did not fail.

Table 1
Test matrix

	Material	Tem (K)	Stress (MPa)	Time to fracture (min)
1	Al pure	523	25	120.3
2	Al pure	573	25	51.0
3	Al pure	623	25	1.2
4	Al pure	523	20	No fracture
5	Al pure	573	20	119.5
6	Al pure	623	20	20.0
7	Al – Al_4C_3	573	25	No fracture
		623	25	No fracture
		673	25	No fracture
		723	25	No fracture
		773	25	No fracture
		773	30	No fracture
		823	35	No fracture
		823	40	2.0

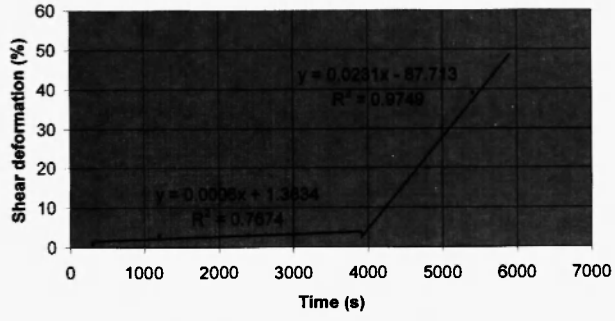

Fig. 8: Pure Al specimen at 523 K, 25 MPa

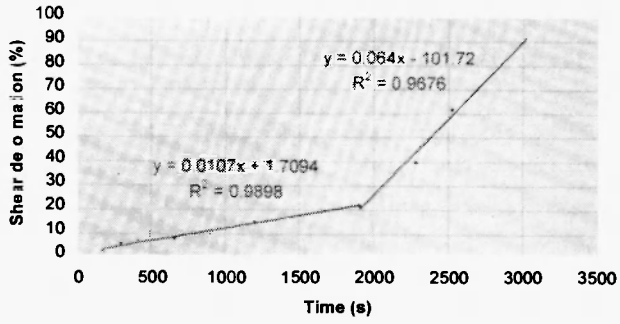

Fig. 9: Pure Al specimen at 573 K, 25 MPa

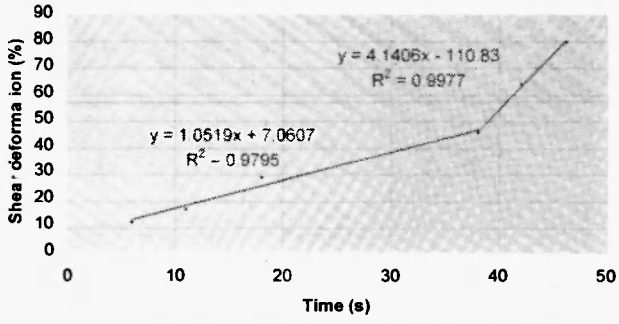

Fig. 10: Pure Al specimen at 623 K, 25 MPa

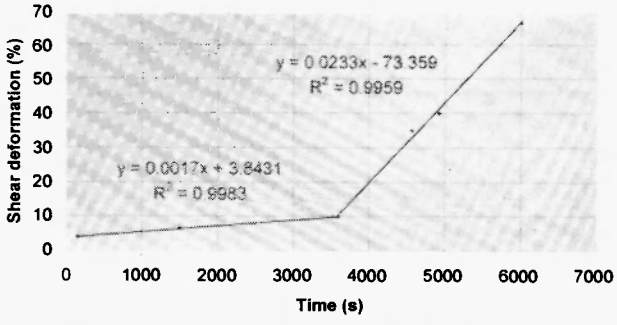

Fig. 11: Pure Al specimen at 573 K, 20 MPa

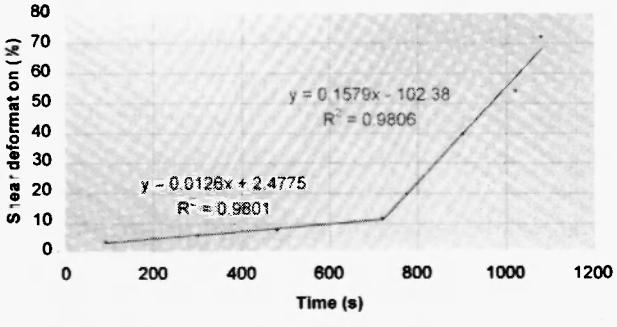

Fig. 12: Pure Al specimen at 623 K, 20 MPa

The composite Al–Al_4C_3 was first tested at 25 MPa and 573 K. It was decided that since its shear creep

properties have never been described in the bibliography the temperature and / or stress would be raised progressively depending on the observed behaviour of the material. After 60 min of loading at 573 K and 25 MPa with negligible deformation the temperature was increased to 623 K while maintaining the same stress level for another 60 min. The temperature was further increased to 673 K for 45 min and 723 K for another 45 min and after 22 minutes of loading at 723 K and 25 MPa some surface cracks appeared in the gage area (center) of the specimen where the uniform pure shear field is developed. These cracks had a tendency to appear and re-appear as the scale was removed, leading to the assumption that they were not deep cracks running inside the material but rather surface cracks of the oxide layer formed as the substrate was deforming due to creep. As the specimen did not show accelerated creep behaviour, the temperature was further increased to 773 K and the loading was kept at 25 MPa for another 60 min.

Despite this increase in temperature the creep did not advance as expected, so the stress level was increased according to the following scheme:

- 30 MPa at 773 K for 20 min. No significant creep was observed.
- 35 MPa at 773 K for 20 min. No significant creep was observed.
- 40 MPa at 773 KC for 2 min. The specimen failed unexpectedly after 2 min without any significant plastic deformation.

The creep rates of the Al–Al_4C_3 specimen were calculated and the results are plotted in **Figs. 13** and **14** with the corresponding ones for the pure aluminum in comparison.

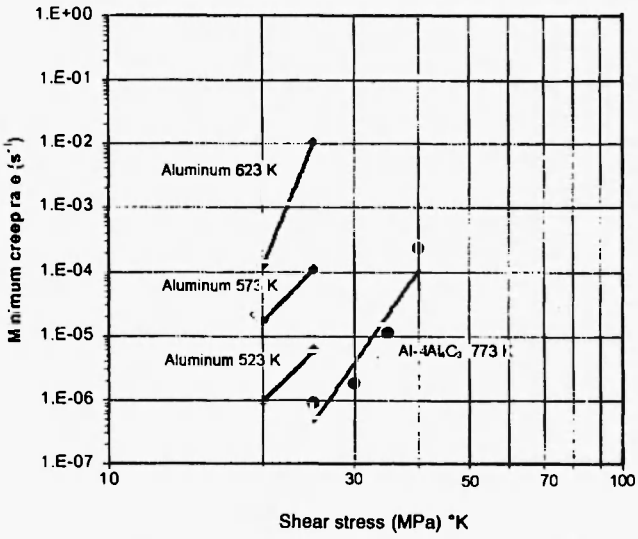

Fig. 13: Shear creep rate vs temperature for Al and Al-Al_4C_3 specimens at various stress levels

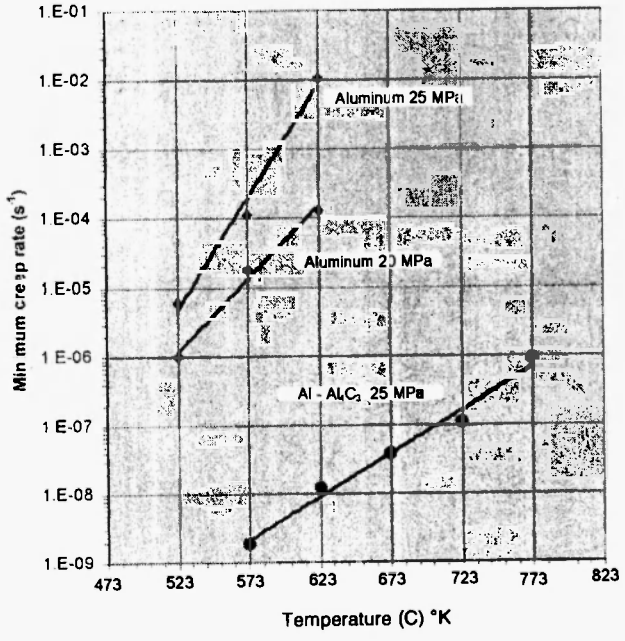

Fig. 14: Shear creep rate vs shear stress for Al and Al-Al_4C_3 specimens at various temperatures

6. CONCLUSION

The conclusions that can be drawn from the test results are the following:

- The shear strain field was uniform in all photographs even at high shear strains (deformations) (Fig. 2). Therefore the assumption of pure shear even at high strains was correct.
- The effect of the temperature dependent activation energy in pure aluminum specimens was important as the creep resistance (time to failure at a given stress level) was considerably different among specimens No. 1, 2 and 3 loaded at 25 MPa and No. 4, 5, 6 at 20 MPa.

- The aluminum carbide MMC exhibited a remarkable creep resistance some orders of magnitude more than the unalloyed aluminum. This material is promising to be used in applications requiring high creep resistance at elevated temperatures such as internal combustion engines pistons and blocks.

ACKNOWLEDGEMENT

The authors wish to acknowledge that the above-presented research was funded under the "Access to Research Infrastructures" programme of the European Commission, Contract No. HPRI-CT-2002-00185 and the Slovak Agency for Science VEGA, Contract No. 2/5142/25.

REFERENCES

1. M. Besterci and J. Ivan, *J. Material Science Letters* **15**, 2071 (1996).
2. M. Besterci, M. Slesár and L. Kováč, *High Temperature Materials and Processes* **16**, 133 (1997).
3. M. Besterci and J. Ivan, *J. Material Science Letters* **17**, 773 (1998)
4. M. Besterci and J. Čadek, *High Temperature Materials and Processes* **23** (1), 51 (2004).
5. M. Besterci, J. Ivan and L. Kováč, *Materials Letters* **46,** 181 (2000).
6. X. Wu, S. W. Holmes and A. K. Ghosh, *Acta Metalurgica et Materialia* **42** (6), 2069 (1994).
7. G. Eggeler and A. Dlouhy, *Physica Status Solidi A* **149** (1), 349 (1995).
8. C. Mayr, G. Eggeler and A. Dlouhy, *Mat. Science and Eng. A* **207** (1), 51 (1996).
9. K. H. G. Ashbee, *J. Material Science Letters* **16** (8), 601 (1997).
10. Z. F. Yue, *Materials at High Temperatures* **18** (3), 171 (2001).
11. Z. F. Yue, H. M. Probst and G. Eggeler, *Mat. Wissenschaft und Werkstofftechnik* **33**, (7), 404 (2002).
12. P. Michelis and P. Nicolaou, in: *Proceedings of the "European Conference on Spacecraft Structures, Materials and Mechanical Testing"*, Braunschweig, Nov. 4-6, 1998.
13. N. Iosipescu, *Journal of Materials* **2** (3), 537 (1967).
14. J. Morton, H. Ho, M. Tsai and G. Farley, *Journal of Composite Materials* **26** (5), 708 (1992).